Emerging materials for microelectromechanical systems at elevated temperatures

Jessica A. Krogstad
Mechanical Engineering Department, Johns Hopkins University, Baltimore, Maryland, USA

Chris Keimel
GE Global Research, Niskayuna, New York, USA

Kevin J. Hemker[a)]
Mechanical Engineering Department, Johns Hopkins University, Baltimore, Maryland, USA

(Received 15 April 2014; accepted 8 July 2014)

Extension of microelectromechanical systems (MEMS) into more extreme operating conditions will require a wider range of material properties than are currently available in conventional systems. Successful integration of new materials is dependent on concurrent development of compatible fabrication routes and scale appropriate evaluation techniques. This review focuses on emerging material classes that have potential to replace silicon-based MEMS in elevated temperature applications. Basic silicon mechanical properties and micromachining methods are reviewed to provide context for developing material systems such as silicon carbide, silicon carbonitrides, and several nickel-based alloys. Potential improvements in strength, thermal stability, and reliability are juxtaposed with fabrication, reproducibility, and economic feasibility issues that must also be addressed.

I. INTRODUCTION

Microelectromechanical systems (MEMS) have broadened the definition of functional microsystems through integration of mechanical and electronic components within a single structure. The unique capabilities of these systems in combination with the economic advantage of high volume/low unit cost production have expanded the application of MEMS[1] to include devices such as sensors,[2] actuators,[3] micropower generators,[4] chemical reactors,[5] and biomedical devices.[6] Continued diversification of this portfolio is widely anticipated, but predicated on concomitant development of appropriate materials, fabrication technologies, and modeling approaches.

History has shown that MEMS-based devices are becoming more complex. Decades ago, the industry witnessed inkjet print heads, a silicon-based MEMS device with no moving parts containing a heating element and an orifice, transform document printing. In subsequent decades, silicon-based devices became more complex and included moving components that enabled the creation and commercialization of pressure sensors, accelerometers, and gyros. Through miniaturization, improved sensor design and controls, and volume fabrication MEMS-based sensors have made their way into consumer-based products where the sensor is valued for its ability to monitor and control. An emerging opportunity for the miniaturization of sensors and MEMS exists from industrial process controls to the monitoring of residential and commercial spaces as described by the concept of the "Internet of Things".[7] Taking sensors into the often harsh environments (temperatures greater than 200 °C, power levels above 100 W) will require new approaches to MEMS devices and that often begins with identifying the materials to construct these sensors from.

To date, material selection for the structural element of many MEMS devices is limited to a relatively small subset of materials compatible with conventional very-large scale integration fabrication technologies—see Fig. 1, with silicon being the dominant structural material. Suspended silicon or polysilicon elements can be found in most accelerometers and are fabricated through deep reactive ion etching (DRIE) of single-crystalline silicon. Thin film vapor-phase deposited materials like silicon nitride are often used to form thin membranes used for pressure sensors and thermopiles. Other vapor phase deposited materials, though less common, have been used as structural materials including but not limited to SiGe;[8] pure aluminum, copper, gold, and platinum; and silicon carbide, silicon oxide, silicon nitride, and titanium nitride.[3] Alternatively, components can be molded through electrodeposition techniques such as Lithographie Galvanisierung Abformung (LIGA), which is capable of fabricating high-aspect ratio nickel structures appropriate for load bearing roles.[9,10]

[a)]Address all correspondence to this author.
e-mail: hemker@jhu.edu
DOI: 10.1557/jmr.2014.183

 © Materials Research Society 2014

https://doi.org/10.1557/jmr.2014.183 Published online by Cambridge University Press

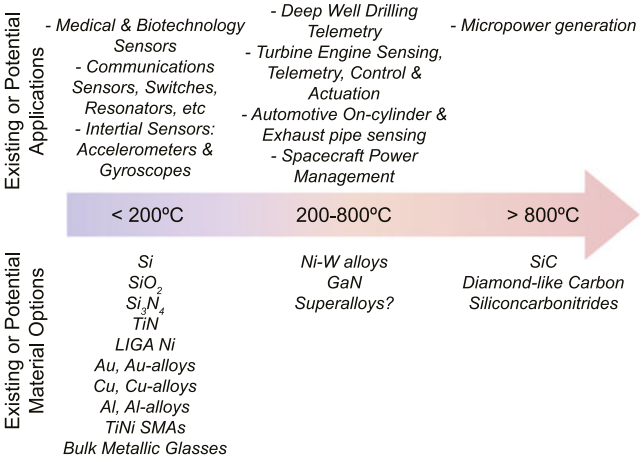


FIG. 1. Examples of existing and potential MEMS materials with respect to different applications and operating regimes.

Despite the ability to create precise and highly complex geometries, the limited range of material properties currently accessible is insufficient for many next generation applications, especially those subject to elevated temperatures. These applications will not only require operation in a harsher environment but will also require MEMS devices that can sustain movement, including surfaces that contact and wear. For example, power MEMS, such as microturbines or miniature internal combustion engines, are regarded as a highly promising frontier in the MEMS community.[11,12] Several examples have been successfully developed; however, these prototypes are severely limited in their capacity and efficiency due to material deficiencies in high temperature mechanical integrity and surface wear.[13,14] Power MEMS have received a considerable amount of attention in the last decade, but even greater potential for expansion of the field exists at more intermediate temperatures (200–800 °C) as illustrated in Fig. 1.[15] Unfortunately, there are fewer economical material choices in this temperature range that exhibit the combination of thermal resistance, creep resistance, mechanical integrity, and wear that will be required for the future sensors.

This has prompted renewed interest in exploring a broader range of structural materials for intermediate and high temperature MEMS applications and has illuminated the challenges associated with integrating new materials into such a highly refined process. In particular, well-defined material properties of materials that can be fabricated and shaped on the microscale and used at elevated temperatures are needed. Reliable definition of such properties is a formidable challenge and further refinement of micromechanical characterization techniques is ongoing.[16] This review was written to highlight emerging materials suitable for elevated temperature MEMSs from the perspective of processing and characterization efforts. Si-based devices are introduced first to provide a baseline for properties, processing routes, and challenges. The following section covers other Si-based material systems that are already in use or under development such as silicon carbide (SiC) and silicon carbonitrides (SiCN). The final section focuses on Ni-based systems including the popular LIGA Ni, efforts to modify pure nickel via vapor phase routes as well as more complex chemistries ranging from Ni–W to conventional Ni-based superalloys.

II. Si-BASED DEVICES

At the core of Si-based MEMS are the well-documented electronic and mechanical properties of single-crystalline and polycrystalline silicon (polysilicon). Integrated circuit (IC) foundries provide access to two key processing routes—surface and bulk micromachining—that have played an important role in the development of Si-based MEMS.[17,18] An attractive aspect of silicon as a mechanical MEMS material is the cross wafer uniformity of its properties and its reproducibility that leads to a level of predictability. Even within these sophisticated fabrication approaches, there remain some challenges specific to MEMS development. Surface micromachining is often limited to a depth of several micrometers, which is insufficient for delivery of compressive or bending mechanical loads or to define the necessary channels or voids necessary for fluidic chemical or biological applications. This can be addressed through bulk micromachining; however, the deep etching process may result in undercutting or preferential etching and ultimately limits the aspect ratio of certain features. Progress towards higher aspect ratios through techniques like DRIE or UV-photolithography is on going.[19–21] Developing the correct combination of materials, etchants and etch stops must be considered for new configurations and are especially important when introducing unconventional complementary metal oxide semiconductor (CMOS) materials. Regardless of these drawbacks, Si-based fabrication methods represent the most complete and well-understood toolset for MEMS development.

Mechanical characterization of single-crystalline and polycrystalline-Si has been the subject of numerous studies; many of the results have been compiled by Sharpe.[16,22] A wide range of values for the elastic modulus was initially published for both materials, but with time both experimental measurements and numerical predictions have converged on a Young's modulus of between 160 and 166 GPa for randomly oriented and <110> textured polysilicon.[23,24] The Young's modulus of single-crystalline Si is a function of orientation and can be predicted from single crystal anisotropic elastic constants. The fracture strength is less well characterized, largely because brittle failure is dependent on flaw size and distribution, which has been shown to vary significantly

https://doi.org/10.1557/jmr.2014.183 Published online by Cambridge University Press

with mask resolution and processing conditions[25] as well as specimen size and geometry.[16] Values between 1.0 and 3.0 GPa are generally accepted.[22]

For many applications, room temperature evaluation is not sufficient. For example, some sensors and actuators for automotive applications may be subjected to temperatures up to 140 °C[26] and other devices that are thermally activated may experience temperatures up to 500 °C. Nakao et al. applied an on-chip tensile testing method on a heated stage to examine the high temperature mechanical properties of single-crystalline Si thin films.[27] The Young's modulus was found to only decrease slightly, but significant changes in the fracture stress were observed above 400 °C with associated evidence of plasticity. The fracture stress at 500 °C was only 32% of that measured at room temperature. Inelastic behavior was also observed by Sharpe at 670 °C, Fig. 2, in this case using resistive heating.[28] This severe thermal degradation is expected to limit the use of Si in many thermally harsh environments envisioned for future MEMS applications. Furthermore, while fatigue is not generally expected to occur in silicon at room temperature under operating stresses of 2 GPa,[29,30] it has been reported in polysilicon[31–33] and may be further accelerated under more aggressive chemical or thermal environments.[34]

III. OTHER Si-BASED MATERIAL SYSTEMS

Several other Si-based materials are commonly found in conventional MEMS. Moreover, ceramics such as silicon dioxide (SiO_2) and silicon nitride (Si_3N_4) are easily deposited and inherent to many IC processes. SiO_2 films are often used as sacrificial layers in the micromachining process as they are easily dissolved in etchants that do not attack polysilicon. SiO_2 may also be used as an etch mask for dry etching of polysilicon.[35] While serving several purposes in the fabrication of complex MEMS, SiO_2 is rarely used as a structural component due to both reduced stiffness (73 GPa) and fracture strength (1 GPa) when compared with polysilicon.[1] The stiffness of silicon nitride (~250 GPa) is on par or a little higher than that of polysilicon, with a slightly higher fracture strength (6 GPa).[36] However, stoichiometric Si_3N_4 thin films are prone to high residual stresses, which limit the thickness to a few hundred nanometers. Si-rich nonstoichiometric silicon nitride films can also be deposited via low pressure chemical vapor deposition (LPCVD) to successfully reduce the residual stresses, but the mechanical performance suffers.[35] As a result, the use of Si_3N_4 remains somewhat limited to membranes and resonators as well as for its thin film properties of electrical isolation and surface passivation.

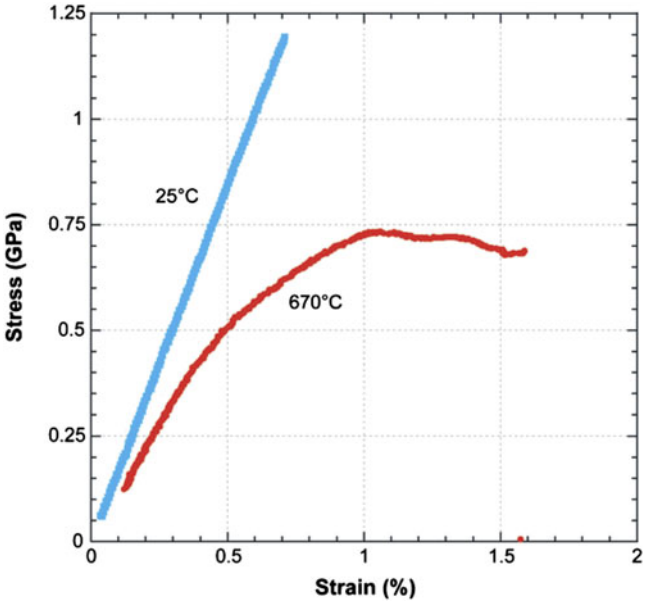


FIG. 2. Stress–strain curves for a polysilicon microtensile sample. Adapted from Ref. 121.

SiO_2 and Si_3N_4 are part of the conventional IC materials set; however, there are several other Si-based materials that are becoming more common in MEMS applications based on processing advantages or their superior mechanical properties and thermal stability. SiGe-based MEMS have generated considerable interest because the processing temperature can be limited to below 450 °C,[8] enabling direct integration with CMOS and even polymer substrates in some cases.[37] CMOS-MEMS integration has many important advantages including noise reduction, improved precision, and even new device applications; however, these are limited typically to the operational temperatures of CMOS of <150 °C. Conversely, silicon carbide (SiC) and polymer-derived silicon carbonitride (Si–C–N) ceramics are two of the most promising Si-based material systems with the potential for elevated temperature operation.

A. SiC

High specific strength and thermal stability make SiC an exciting candidate for high temperature MEMS.[38] Although the fracture strength remains highly dependent on the test configuration and specimen geometry and size, high temperature tensile tests (~1000 °C) have shown that the strength is maintained when compared with room temperature evaluation in the same configuration.[39] A recent computational study by Wang et al. has begun to elucidate some of the fracture mechanisms specific to SiC both at ambient and elevated temperatures, including permanent deformation via bond breaking according to resolved shear stresses on an active slip plane.[40] The wear resistance is also exceptional,[41] enabling SiC as a viable coating material for surfaces that contact and wear. The Young's modulus of SiC can range from 300 to 700 GPa depending on the polymorph and crystallographic

https://doi.org/10.1557/jmr.2014.183 Published online by Cambridge University Press

orientation.[35,42] Hundreds of polymorphs, or polytypes—identical planar arrangement of Si and C but different stacking sequences—have been reported for SiC, but only three crystalline types exist: cubic, hexagonal, and rhombohedral.[43] The only cubic polytype is commonly referred to as 3C-SiC (historically β-SiC). Common hexagonal polytypes are 6H-SiC and 4H-SiC. To date, bulk crystal growth of 3C-SiC is challenging and thus limiting its adaption for electronic devices and sensors. 6H-SiC and 4H-SiC can be fabricated in bulk and small wafers (<100 mm) are available; however, these remain expensive.[44] Homoepitaxy of 6H-SiC on single crystalline wafers is possible, but the more common approach is through heteroepitaxy of 3C-SiC on Si wafers. Polycrystalline SiC (poly-SiC) offers greater flexibility and may be deposited on a wide variety of substrates, including sacrificial SiO_2. The processing temperatures for poly-SiC are also considerably lower, between 200 and 1000 °C as compared with that between 1500 and 1700 °C for deposition of the crystalline polytypes.[41] Furthermore, the texture of poly-SiC can be controlled by controlling the texture of the polysilicon substrate. It has been shown in polysilicon that texture influences important properties such as elastic modulus and thermal conductivity. This is also true for poly-SiC and careful control of crystallographic texture will be required to tailor the performance of a given thin film.[41]

Yet SiC is relatively immature when compared with micromachined silicon and LIGA nickel. Several recent reviews have outlined progress in SiC MEMS, but considerable work remains necessary to realize a larger market share beyond current niche applications including high temperature micromechanical resonators in communication transceivers, pressure sensors in the oil industry, and accelerometers in airplane engines or spacecraft.[38,44,45] Many of these challenges revolve around improving fabrication routes. Chemical vapor deposition (CVD) is used almost exclusively for SiC thin film growth, although several variations exist that are specific to the polytype or application. Atmospheric pressure chemical vapor deposition (APCVD) was one of the first techniques developed for SiC and is still routinely used for both epitaxial and polycrystalline 3C-SiC.[44] Large residual stresses often result from this high temperature process, usually between 1200 and 1360 °C. LPCVD results in a slower growth rate, but can more easily accommodate the thermal stresses in the thin films.[45] Growth of homoepitaxial 6H-SiC or 4H-SiC must be done at very high temperatures between 1500 and 1650 °C, which limits integration into CMOS devices.[44] However, lower temperature (800–1000 °C) LPCVD processes have been developed for polycrystalline 3C-SiC films.[46] Plasma enhanced CVD (PECVD) allows for deposition of amorphous SiC films at substantially lower temperatures (200–400 °C).[47] Amorphous SiC (a-SiC) films can be crystallized by post-deposition annealing, but are commonly deposited as a coating material for various MEMS components. Residual stresses in a-SiC must be carefully controlled through adjustment of deposition parameters and post-deposition annealing.[44]

CVD is generally compatible with masking schemes to develop patterned depositions. Unfortunately, due to the chemical inertness of SiC—which for other practical purposes is desirable—typical anisotropic etchants are not effective for traditional surface or bulk micromachining. Freestanding or partially released components, such as diaphragms and cantilevers, can be fabricated through deposition on sacrificial substrates that can be bulk micromachined. Surface micromachining can be achieved in some cases when plasma-based dry etching is used, for example, see Fig. 3. Fluorine-based gas mixtures are key to the process, which can be slow and lead to anisotropic etch profiles.[45] Other processes such as photoelectrochemical etching[48] and DRIE have also been developed for improved dimensional control and greater aspect ratios.[49] The latter is more commonly applied to Si, which is used as a sacrificial mold for deposited poly-SiC.[44] In an early example of this technique, Rajan et al. fabricated a fuel atomizer for gas turbine applications.[50] Other micromolding techniques using preceramic polymers, such as polycarbosilane, have been developed to create high aspect ratio MEMS components. Slip casting the preceramic in a SU-8 mold followed by pyrolysis and repeated infiltration of the polymer precursor (known as the polymer infiltration and pyrolysis (PIP) process) is necessary to achieve acceptable densities.[51,52] Micromolding is gaining popularity, but is not without its drawbacks as will be discussed in more detail in the following section.

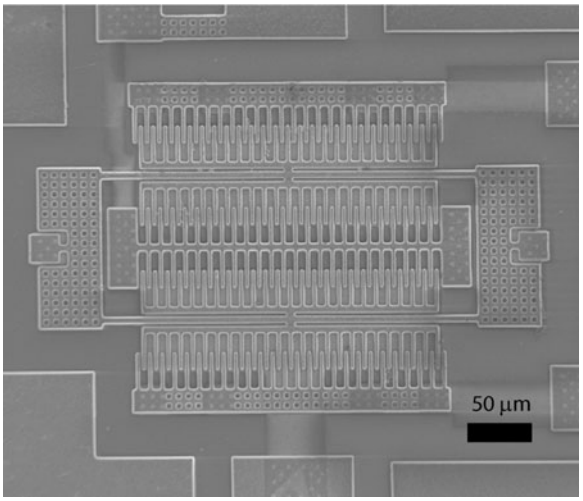


FIG. 3. A balanced-mass double-ended tuning fork fabricated from 3C-SiC deposited on a silicon substrate and shaped via surface micromachining routes. Courtesy of Azevedo et al.[122]

https://doi.org/10.1557/jmr.2014.183 Published online by Cambridge University Press

Challenges remain for SiC in MEMS devices, but the technology is making great strides in becoming more commercially viable. One burgeoning area involves integration of SiC and group III nitrides, such as GaN or AlN.[3,53] These nitrides offer an exciting array of functionality while maintaining chemical inertness and thermal stability. This coupling may represent a whole new subset of harsh environment MEMS with further processing refinements. While a significant effort has focused on the use of these wide-band gap semiconductors as biological or chemical gas sensors,[54] several devices ranging from simple cantilevers[55] to micromirror arrays,[56] resonating strain sensors (e.g., Fig. 4),[57] and gyroscopes[58] have been demonstrated. Pearton et al.[59] provide a more detailed discussion of the available processing routes, functional advantages, and specific device performance.

Finally, while many of the properties of SiC have been trumpeted as ideal for high temperature MEMS, the specific application is still very important. Take the relatively high thermal conductivity (320–490 W/m K) as an example. This is ideal for rapid heat transport but more problematic when thermal isolation is key to microsystem efficiency. In a recent report by Liamini et al. detailing the design methodology for a Rankine microturbine, Si and SiC were all but ruled out from the material selection due to the inability to sustain large thermal gradients (~100 °C/mm) despite relatively mature manufacturing technologies.[14] This is only one example of the trade offs between material properties and manufacturability and emphasizes that a single material system is unlikely to meet all of the needs of the many foreseeable high temperature MEMS applications.

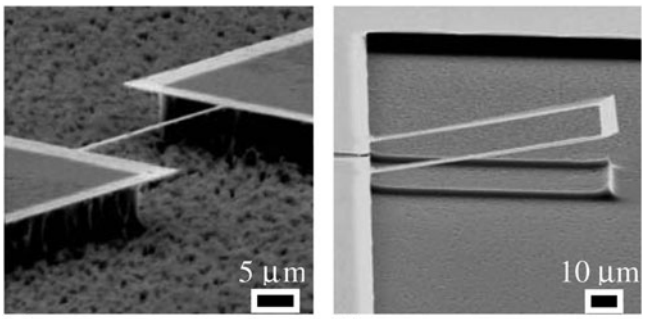


FIG. 4. SEM images of resonant beams fabricated from AlN in a (a) nanoresonator and (b) "U" shaped configuration.[123]

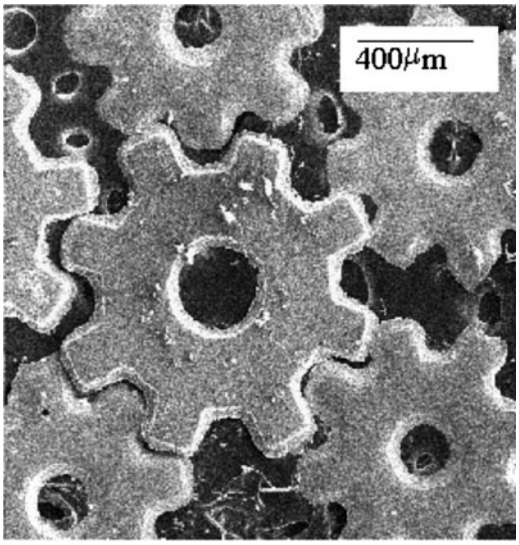


FIG. 5. Example SiCN gear structure approximately 50 μm thick fabricated using microforged molds.[71]

B. SiCN

Much like SiC, silicon carbonitrides (SiCN) combine several desirable properties for high temperature MEMSs including thermal stability, high stiffness, creep resistance, and oxidation resistance.[60,61] This is true for many ceramic systems; however, SiCN has the advantage of fabrication through preceramic polymers such as polyorganosilazanes. Polymer-derived ceramics (PDCs) were developed in the 1960s and 70s[62] but were largely brought to the attention of the MEMS community by Liew et al. in the early 2000s.[60,63,64]

The ability to fabricate high aspect ratio components is one of the many advantages of PDCs—see Fig. 5. This includes methods to bond components together resulting in a monolithic structure.[64] However, the properties of a PDC MEMS component are strongly influenced by the processing conditions, e.g., low density or large flaw size distribution can dramatically reduce the strength. Many processing routes have been proposed to maintain the required high aspect ratios without sacrificing reliability and mechanical integrity. These methods must also conform to common MEMS processes. Liew et al. originally proposed the use of UV-photolithographic techniques and traditional SU-8 mold to fabricate dense near-net shape components.[64] To effectively fill the molds, the preceramic polymers must have a relatively low viscosity, which is often achieved through low solids loading. Unfortunately, such low solids content results in shrinkage of up to 30%. This large degree of shrinkage must be accounted for in the component design, but more importantly during the drying, cross-linking, and pyrolysis steps interactions between the shrinking preceramic polymer and the mold walls or substrate can lead to the build up of stress and result in microcracking or delamination. In some cases, structures with a diameter <50 μm and thinner than 20 μm can be pyrolyzed on the substrate without damage.[65] Liew et al.[63] and Schulz[66] present a more comprehensive overview of the microcasting process advantages and challenges.

Several methods have been developed to reduce damage due to shrinkage. Use of different ceramic powder filler materials is one common route. Active filler materials

https://doi.org/10.1557/jmr.2014.183 Published online by Cambridge University Press

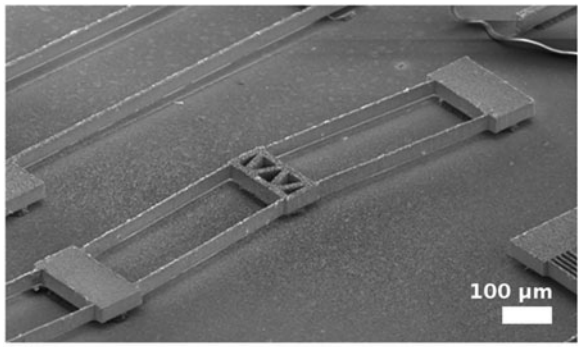
(B, Si, Al, Ti, Mo, etc.) can react with the polymer decomposition products to form new phases. The resulting volume expansion effectively counteracts shrinkage and leads to near-net-shape ceramic components.[67,68] If the filler material is chosen carefully, this may also improve properties such as electrical conductivity.[69,70] However, changes in the scattering/absorption behavior must be accounted for in direct lithography processes when using filler materials.[66] A microforging process, which removes the green-body from the mold prior to drying and pyrolysis, was proposed by Liu et al.[71] In this method, the components are microcast on a NaCl substrate, the mold is removed and a sacrificial wax handling plate is used to transfer the components to the heat treatment processes, during which the wax melts away and freestanding components are left. At this point, the freestanding components must be manually placed within the MEMS device. This is a nontrivial task that may lead to warping and will greatly increase cost by eliminating massively parallel processing. Bright et al. pursued a similar route using hot isostatic pressing.[69] Soft lithography methods,[72,73] PECVD,[74] and even sputtering[75,76] have also been explored, but these ultimately limit the potential aspect ratio.

To date, most PDC work on high temperature MEMSs has focused on commercially available forms of Si–C–N precursors. The motivation for this is clear—any new processes must be economically viable and competitive with other mature MEMS processing routes. However, many other precursor-derived ceramic systems have been studied and shown to have promising mechanical properties.[61] A potentially large design space for tailoring specific properties exists if some of the aforementioned processing challenges can be overcome.

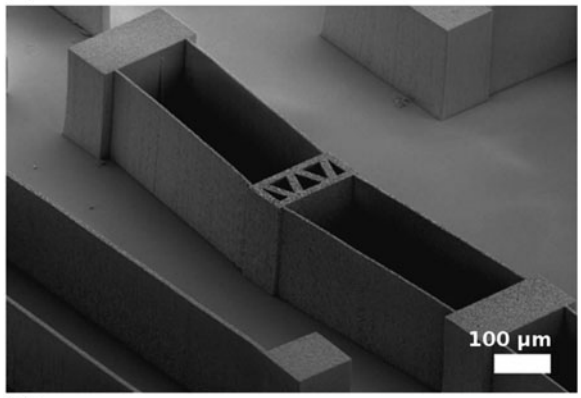
IV. Ni-BASED MATERIAL SYSTEMS

MEMS structures must be mechanically robust. To-date, MEMS designers have relied on the fact that IC-based MEMS fabrication processes significantly mitigate the introduction of critical flaws that would be detrimental to intrinsically brittle materials like the previously discussed Si-based materials.[16] By contrast, the intrinsic strength and toughness of metallic alloys are dramatically higher and can easily be tailored. The push for MEMS materials that can be reliably implemented in extreme environments and at elevated temperatures calls for the reexamination and development of metallic alloys that possess a broad range of tailorable properties and can be fabricated and shaped on the microscale. Silicon has succeeded in creating classes of two-dimensional sensors, such as accelerometers and gyroscopes, through precise thin film polysilicon deposition and processing. However, polysilicon is limited by its deposited film stress to a thickness of a few tens of micrometers in a single layer or 2–3 integrated thin layers. The connectivity of industrial systems will drive future generations of MEMS sensors and actuators that will operate at temperatures >150 °C, will require 10x improvements in sensitivity as well as stability and drift minimization. New structural materials such as metal alloys are poised to meet these sensor demands through both material properties as well as processing techniques that can enable three-dimensional MEMS sensors and high aspect ratio features—e.g., through use of carbon nanotube (CNT) scaffolding as demonstrated by Hutchison et al. in Fig. 6.[77] The integration of metals and alloys into MEMS structures would also provide a much wider design space with regard to density, electrical and thermal conductivity, and even reflectance.

The wide-spread use of electrodeposited Ni in LIGA micromolding and microstructure applications and the development of multicomponent Ni-based superalloys as elevated temperature macroscale structural materials make Ni-based materials an obvious starting point for high temperature MEMS applications. The overarching challenge is to develop processing routes that allow for both microscale shaping and the development of complex alloys and material microstructures.



(a)



(b)

FIG. 6. An example of a high aspect ratio 3D structure fabricated from a CNT-silicon nitride composite process. (a) released bistable mechanism (BSM); (b) unreleased CNT-silicon nitride composite BSM. Courtesy of Hutchison et al.[77]

https://doi.org/10.1557/jmr.2014.183 Published online by Cambridge University Press

A. LIGA Ni

Development of the LIGA technique over the last several decades has enabled microfabrication of complex structural elements and molds that are relatively thick yet capable of maintaining a high aspect ratio—see Fig. 7.[78] Ni is very easily electrodeposited and LIGA Ni components have received considerable attention. When the grain size is properly controlled to a nanometer scale (e.g., <100 nm[79]) and texture accounted for,[80] the strength of electroplated Ni increases dramatically over that of the bulk metal. In addition to being highly sensitive to the exact deposition conditions,[9] the thermal stability of such a fine-grained, nonequilibrium microstructure is unfortunately low. Rapid softening has been observed during both annealing[80] and elevated temperature loading.[10] Significant creep has also been observed at room temperature.[81] This instability has been attributed to the mobility of high energy grain boundaries formed through electrodeposition, and it has been suggested that if properly conditioned through cyclic loading, the grain boundaries may relax without significant grain coarsening and loss of mechanical strength at ambient temperature.[81,82] However, the application of nominally pure LIGA nickel in load bearing configurations is expected to be quite limited on the basis that most conventional MEMS packaging processes use temperature excursions beyond the threshold for microstructural stability.

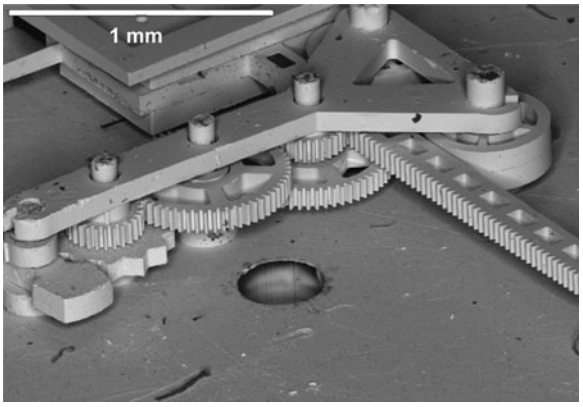


FIG. 7. An example LIGA Ni microsystem.[9]

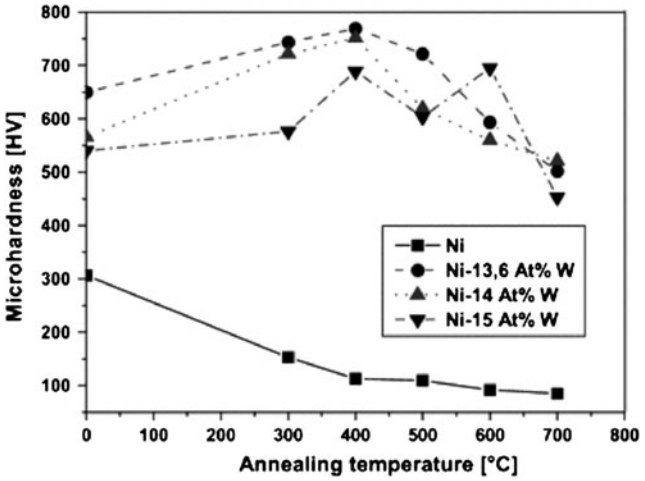


FIG. 8. Comparison of microhardness data for LIGA Ni and several LIGA Ni–W alloys after a 2 h anneal at elevated temperature.[92] Reprinted with permission.

B. Binary Ni alloys

Considerable effort has been made to improve the thermal stability of the nanograin structure of electrodeposited nickel films. One promising route is through the introduction of alloying elements, such as iron,[83] tungsten,[84] cobalt,[85,86] or manganese.[86–89] Table I summarizes the mechanical properties of several binary Ni-alloys in comparison with pure LIGA Ni.[85,86,90–92] The as-deposited strengths are quite good; however, challenges with sulfur grain boundary segregation and grain coarsening limit the utility of the Ni–Fe[85] and Ni–Co[86,90] systems at elevated temperatures. While Ni–Mn performs well even after thermal annealing, maintaining a significant fraction of the as-deposited strength and a very respectable ductility,[86] the magnetic properties and lower density of this alloy have limited its implementation. This leaves the Ni–W system, which has somewhat limited ductility in the as-deposited condition[93] but has excellent thermal stability and high density.[91,92]

Originally considered for coating applications due to its superior corrosion and wear resistance,[94–96] electrodeposited nanocrystalline Ni–W is a promising candidate for structural elements in MEMS.[91,92,97] Figure 8, from Haj-Taieb et al.,[91] illustrates the improvement in mechanical performance at elevated temperatures. The strength of LIGA Ni was largely attributed to the fine grain size achievable through electrodeposition.[79] However, this behavior has been shown to peak at some critical grain size. Schuh, Nieh, and Iwasaki[96] demonstrated that such a breakdown in strengthening behavior may be due to a diffusive mechanism in which case, the addition of alloying elements with limited diffusivity—such as W in Ni—would suppress this critical grain size and further increase the strength. Although the traditional (e.g., Fleischer model[98]) calculated solid solution strengthening contribution of W in Ni is quite low, the same group later presented a new strengthening mechanism based on dislocation pinning at grain boundaries.[99] The efficiency of this mechanism is dependent on the global properties of a material including shear modulus and Burgers vector, both of which may be significantly impacted by the addition of solute atoms like W. Furthermore, subtle grain boundary segregation of W also contributes to the stability of the fine microstructures necessary for this nanocrystalline strengthening mechanism to dominate.[100] The added microstructural stability

https://doi.org/10.1557/jmr.2014.183 Published online by Cambridge University Press

TABLE I. Comparison of the mechanical properties of several Ni-binary alloys to pure LIGA Ni.

		Ultimate tensile strength (MPa)		Strain to failure (%)			
	Deposition bath	RT	600 °C	RT	600 °C	Challenges	References
LIGA Ni	Watts bath (+1 g/L saccharin)	1750	50[a]	12	0.04	Grain coarsening, S embrittlement	[86]
	Sulfamate bath	610	420	12.8	>40		[86]
Ni–Fe	Sulfamate bath	~1800	200	~13	0	S embrittlement, ferromagnetic	[85]
Ni–Co	...	1500	525	12	>30	Grain coarsening, compositional homogeneity, ferromagnetic	[86,90]
Ni–Mn	Sulfamate bath (DC plated)	1630	1350	2.5	7.5	Antiferromagnetic	[86]
Ni–W (15%)	Ammonia-citrate bath	1050	1800	0.5	2	...	[91,92]

[a]Data collected after 1 h anneal at 500 °C.

of subtle grain boundary solute segregation is ultimately limited to temperatures below 500 °C where normal grain coarsening ensues[101] and due to the onset of ordering (to Ni_4W-phases) as 700 °C is approached.[95,102]

Other schemes including the inclusion of WO_4 particles in electrodeposited Ni films[103] and the addition of P[104] or Fe[105] to electrodeposited Ni–W alloys have also been explored in the context of wear- and corrosion-resistant coatings and have not been investigated as freestanding films.

C. Vapor phase aluminization of LIGA Ni structures

Electrodeposition is easily adaptable to conventional microfabrication methods but significantly limits compositional flexibility to one or two component alloys and the deposition parameters must be carefully tailored for each new composition. Moreover, certain elements such as aluminum cannot be electrodeposited from aqueous solutions. Important classes of structural materials, e.g., nickel aluminide intermetallics and Ni-based superalloys, are excluded on this basis and alternative efforts to modify LIGA Ni with Al are required.

Vapor-phase modification of bulk Ni-based superalloys is a common approach for application of protective barrier coatings on structural components subjected to extreme environments. Development of a β-NiAl intermetallic bond coat is a typical goal of this process; however, routes for chromizing as well as siliconizing have also been developed.[106–108] Pack aluminization has also been applied to much finer structures where the thickness of the deposited layer is on the same length scale as the structure itself. In these cases, an additional homogenization step results in a uniform Ni–Al alloy[109,110] or a desired two-phase γ/γ' microstructure with the corresponding high temperature mechanical stability.[111,112]

Conversion of LIGA Ni MEMS components to a Ni-rich two-phase (γ–γ') superalloy microstructure via pack aluminization has recently been explored by Burns et al.[113] The aluminized components showed significantly improved microstructural stability. Furthermore, the trimodal distribution of γ'-precipitates resulted in marked improvements in both room and elevated temperature strength. These binary microsamples suffered from elevated temperature grain boundary oxidation and embrittlement,[114] but this embrittlement can be overcome with an additional chromizing step as demonstrated by Choe and Dunand.[115] The full potential of nickel aluminides as structural MEMS materials appears promising, but the feasibility of a multistep homogenization process will face many of the same challenges as the silicon carbonitrides and must be assessed in the context of rapid, reliable, and compatible MEMS production.

D. Ni-based superalloys

The precipitation strengthening and oxidation resistance afforded by Al- and Cr-vapor phase modification of LIGA Ni is a first step toward approaching the high temperature mechanical performance of traditional Ni-based superalloys at the MEMS scale. Optimal performance of such Ni-based superalloys is dependent on contributions from a host of alloying elements, which cannot feasibly be incorporated via electrodeposition or pack aluminization. Sputtering provides an alternative fabrication method that has already been integrated into many MEMS processing routes and is capable of maintaining the complex compositions of a Ni-based superalloy. Sputtered binary Ni–W alloys have already been discussed and demonstrate compositional flexibility beyond equilibrium solubility levels as well as greater microstructural control.[99,102] Nanocrystalline superalloy coatings deposited via sputtering have also been explored for corrosion[116] and oxidation protection.[116–118]

Preliminary efforts to sputter first generation Ni-based superalloys in the context of freestanding films for MEMS applications have been undertaken by Burns et al.[119] As was observed for the corrosion and oxidation applications, the influence of the initial nonequilibrium

https://doi.org/10.1557/jmr.2014.183 Published online by Cambridge University Press

microstructure of the sputtered films played an important role in dictating the properties of the thick films. The initial yield strength of the as-deposited films both at room temperature and elevated (700 °C) temperature was significantly enhanced relative to the bulk alloy. This demonstrated that the initially fine microstructure was stable even at 700 °C. However, the homogenous as-deposited films did not take advantage of the precipitation strengthening mechanism that contributes to the high temperature mechanical behavior of typical Ni-based superalloys. The conventional annealing profiles for Inconel 718 require a combination of 16 h above 600 °C. Initially, this may be seen as a hurdle for MEMS incorporation, but Burns et al.[113] also demonstrated that the prevalence of grain boundaries changed the precipitation pathways in the sputtered alloy. Instead of developing the expected metastable γ''-phase, the equilibrium δ-phase was observed. This is effectively indicative of an overaged microstructure, suggesting accelerated phase evolution kinetics. Both the prevalence of heterogeneous nucleation sites, e.g., grain boundaries, and the initial stress state of Inconel 718 have previously been shown to influence the position of time–temperature–transformation (TTT) curves.[120] Given that both of these variables can be tuned through the sputtering processing, this may lead to opportunities to reduce the time and temperatures necessary to develop the desired two-phase microstructure and activate precipitation strengthening in specific thin film alloys.

V. CONCLUDING REMARKS

Silicon-based MEMSs are at the core of the rapidly expanding microsystems industry. Predictable properties and streamlined fabrication methods assure that Si will continue to play an important role in the industry. However, a broader spectrum of MEMS materials would offer a wider range of functionality and fuel a greatly expanded assortment of MEMS applications especially in extreme environments. Several candidate material systems including silicon carbide (SiC), silicon carbonitrides (SiCN), and nickel-based alloys have been reviewed based on their potential for high temperature MEMS integration. SiC is the most mature of these technologies. Impressive thermal stability and wear resistance are among the attractive properties of SiC. Efforts to reduce cost and to improve control of aspect ratio and residual stress in deposited structures will further improve the feasibility of SiC. The high thermal conductivity of SiC is attractive for many applications but not all—in these cases, SiCNs are a viable alternative if component shrinkage and methods for reliable placement can be developed. Metallic systems may provide the greatest potential to tune strength and reliability of MEMS components at elevated temperature. Simple electrodeposited binary nickel alloys such as Ni–W have already demonstrated high strength and thermal stability up to 500 °C. Increasingly complex alloys provide the opportunity to improve upon high temperature corrosion and oxidation resistance, dimensional stability, and damage tolerance (cyclic and static). Processing methods such as sputtering also provide much needed flexibility to tune grain size and residual stress, which are not only important to dimensional tolerances but also offer opportunities to accelerate microstructure development necessary for optimal high temperature mechanical properties.

Each of these new MEMS materials must overcome unique challenges before successful integration. However, the driving force for continued expansion of the MEMS industry into more extreme environments is likely to provide the necessary impetus for continued development of these and future MEMS materials.

REFERENCES

1. S.M. Spearing: Materials issues in microelectromechanical systems (MEMS). *Acta Mater.* **48**(1), 179–196 (2000).
2. M. Esashi: Revolution of sensors in micro-electromechanical systems. *Jpn. J. Appl. Phys.* **51**(8), 8 (2012).
3. S.A. Wilson, R.P.J. Jourdain, Q. Zhang, R.A. Dorey, C.R. Bowen, M. Willander, Q.U. Wahab, S.M. Al-hilli, O. Nur, E. Quandt, C. Johansson, E. Pagounis, M. Kohl, J. Matovic, B.R. Samel, W. van der Wijngaart, E.W.H. Jager, D. Carlsson, Z. Djinovic, M. Wegener, C. Moldovan, R. Iosub, E. Abad, M. Wendlandt, C. Rusu, and K. Persson: New materials for micro-scale sensors and actuators: An engineering review. *Mater. Sci. Eng., R* **56**(1–6), 1–129 (2007).
4. L. Weiss: Power production from phase change in MEMS and micro devices, a review. *Int. J. Therm. Sci.* **50**(5), 639–647 (2011).
5. K.F. Jensen: Silicon-based microchemical systems: Characteristics and applications. *MRS Bull.* **31**(2), 101–107 (2006).
6. J. Ponmozhi, C. Frias, T. Marques, and O. Frazao: Smart sensors/actuators for biomedical applications: Review. *Measurement* **45**(7), 1675–1688 (2012).
7. K. Ashton: That Internet of Things Thing: In the real world, things matter more than ideas. *RFID J.* **22**, June, 2009.
8. A. Witvrouw: CMOS-MEMS integration today and tomorrow. *Scr. Mater.* **59**(9), 945–949 (2008).
9. T.E. Buchheit, D.A. LaVan, J.R. Michael, T.R. Christenson, and S.D. Leith: Microstructural and mechanical properties investigation of electrode posited and annealed LIGA nickel structures. *Metall. Mater. Trans. A* **33**(3), 539–554 (2002).
10. H.S. Cho, K.J. Hemker, K. Lian, J. Goettert, and G. Dirras: Measured mechanical properties of LIGA Ni structures. *Sens. Actuators, A* **103**(1–2), 59–63 (2003).
11. S.A. Jacobson and A.H. Epstein: An informal survey of power MEMS. In *Proceedings of the International Symposium on Micromechanical Engineering*, Vol. **12**, 2003; pp. 513–519.
12. S.K. Chou, W.M. Yang, K.J. Chua, J. Li, and K.L. Zhang: Development of micro power generators - A review. *Appl. Energy* **88**(1), 1–16 (2011).
13. A.H. Epstein: Millimeter-scale, MEMS gas turbine engines. In *Proceedings of ASME Turbo Expo Collocated with the 2003 International Joint Power Generation Conference*, American Society of Mechanical Engineers, 2003; pp. 669–696.
14. M. Liamini, H. Shahriar, S. Vengallatore, and L.G. Fréchette: Design methodology for a Rankine microturbine: Thermome-

https://doi.org/10.1557/jmr.2014.183 Published online by Cambridge University Press

chanical analysis and material selection. *J. Microelectromech. Syst.* **20**(1), 339–351 (2011).
15. P.G. Neudeck, R.S. Okojie, and C. Liang-Yu: High-temperature electronics - A role for wide bandgap semiconductors? *Proc. IEEE* **90**(6), 1065–1076 (2002).
16. K.J. Hemker and W.N. Sharpe: Microscale characterization of mechanical properties. *Annu. Rev. Mater. Res.* **37**, 93–126 (2007).
17. M.J. Madou: *Fundamentals of Microfabrication: The Science of Miniaturization* (CRC Press, 2002).
18. K.D. Wise: Special issue on integrated sensors, microactuators, & microsystems (MEMS). *Proc. IEEE* (1998).
19. S.R. Jensen, A.D. Yalçinkaya, S.R. Jacobsen, T. Rasmussen, F.E. Rasmussen, and O. Hansen: Deep reactive ion etching for high aspect ratio microelectromechanical components. *Phys. Scr.* **2004**(T114), 188 (2004).
20. M. Esashi and T. Ono: From MEMS to nanomachine. *J. Phys. D: Appl. Phys.* **38**(13), R223–R230 (2005).
21. B.Q. Wu, A. Kumar, and S. Pamarthy: High aspect ratio silicon etch: A review. *J. Appl. Phys.* **108**(5), 20 (2010).
22. W.N. Sharpe: Mechanical properties of MEMS materials. In *The MEMS Handbook*, Vol. **3**, 2002; pp. 1–33.
23. W.N. Sharpe, Jr., Y. Bin, R. Vaidyanathan, and R.L. Edwards: Measurements of Young's modulus, Poisson's ratio, and tensile strength of polysilicon. In *Proceedings of the Tenth IEEE International Workshop on Microelectromechanical Systems, MEMS '97*, 1997; pp. 424–429.
24. S. Jayaraman, R. Edwards, and K. Hemker: Relating mechanical testing and microstructural features of polysilicon thin films. *J. Mater. Res.* **14**(03), 688–697 (1999).
25. F.W. DelRio, L.H. Friedman, M.S. Gaither, W.A. Osborn, and R.F. Cook: Decoupling small-scale roughness and long-range features on deep reactive ion etched silicon surfaces. *J. Appl. Phys.* **114**(11), 113506 (2013).
26. R. Müller-Fiedler and V. Knoblauch: Reliability aspects of microsensors and micromechatronic actuators for automotive applications. *Microelectron. Reliab.* **43**(7), 1085–1097 (2003).
27. S. Nakao, T. Ando, M. Shikida, and K. Satol: Mechanical properties of a micron-sized SCS film in a high-temperature environment. *J. Micromech. Microeng.* **16**(4), 715–720 (2006).
28. W.N. Sharpe: Tensile testing of MEMS materials at high temperatures. In *Advances in Experimental Mechanics IV*, Vol. **3–4**, J.M. Dulieu-Barton and S. Quinn, eds., Trans Tech Publications Ltd: Stafa-Zurich, 2005; pp. 59–64.
29. T. Ando, M. Shikida, and K. Sato: Tensile-mode fatigue testing of silicon films as structural materials for MEMS. *Sens. Actuators, A* **93**(1), 70–75 (2001).
30. C.L. Muhlstein, R.T. Howe, and R.O. Ritchie: Fatigue of polycrystalline silicon for microelectromechanical system applications: Crack growth and stability under resonant loading conditions. *Mech. Mater.* **36**(1–2), 13–33 (2004).
31. D.H. Alsem, O.N. Pierron, E.A. Stach, C.L. Muhlstein, and R.O. Ritchie: Mechanisms for fatigue of micron-scale silicon structural films. *Adv. Eng. Mater.* **9**(1–2), 15–30 (2007).
32. H. Kahn, A. Avishai, R. Ballarini, and A. Heuer: Surface oxide effects on failure of polysilicon MEMS after cyclic and monotonic loading. *Scr. Mater.* **59**(9), 912–915 (2008).
33. H. Kahn, R. Ballarini, and A. Heuer: Dynamic fatigue of silicon. *Curr. Opin. Solid State Mater. Sci.* **8**(1), 71–76 (2004).
34. A.D. Romig, M.T. Dugger, and P.J. McWhorter: Materials issues in microelectromechanical devices: Science, engineering, manufacturability and reliability. *Acta Mater.* **51**(19), 5837–5866 (2003).
35. C.A. Zorman and M. Mehregany: Materials for microelectromechanical systems. *The MEMS Handbook* (CRC Press, 2001).
36. W.N. Sharpe: Mechanical properties of MEMS materials. *The MEMS Handbook* (CRC Press, 2001).
37. J. El-Rifai, S. Sedky, R. Van Hoof, S. Severi, D. Lin, S. Sangameswaran, R. Puers, C. Van Hoof, and A. Witvrouw: SiGe MEMS at processing temperatures below 250 °C. *Sens. Actuators, A* **188**, 230–239 (2012).
38. P.M. Sarro: Silicon carbide as a new MEMS technology. *Sens. Actuators, A* **82**(1–3), 210–218 (2000).
39. W.N. Sharpe, Jr., G. Beheim, N. Nemeth, L. Evans, and O. Jadaan: Strength of single-crystal silicon carbide microspecimens at room and high temperature. In *Proceedings of the 2005 SEM Annual Conf.*, Portland, OR, 2005.
40. W-X. Wang, L-S. Niu, Y-Y. Zhang, and E-Q. Lin: Tensile mechanical behaviors of cubic silicon carbide thin films. *Comput. Mater. Sci.* **62**, 195–202 (2012).
41. M. Mehregany and C.A. Zorman: SiC MEMS: Opportunities and challenges for applications in harsh environments. *Thin Solid Films* **355**, 518–524 (1999).
42. K.M. Jackson: Fracture strength, elastic modulus and Poisson's ratio of polycrystalline 3C thin-film silicon carbide found by microsample tensile testing. *Sens. Actuators, A* **125**(1), 34–40 (2005).
43. M. Mehregany, C.A. Zorman, N. Rajan, and C.H. Wu: Silicon carbide MEMS for harsh environments. *Proc. IEEE* **86**(8), 1594–1610 (1998).
44. C.A. Zorman and R.J. Parro: Micro- and nanomechanical structures for silicon carbide MEMS and NEMS. *Phys. Status Solidi B* **245**(7), 1404–1424 (2008).
45. L. Jiang and R. Cheung: A review of silicon carbide development in MEMS applications. *Int. J. Comput. Mater. Sci. Surf. Eng.* **2**(3), 227–242 (2009).
46. C.R. Stoldt, C. Carraro, W.R. Ashurst, D. Gao, R.T. Howe, and R. Maboudian: A low-temperature CVD process for silicon carbide MEMS. *Sens. Actuators, A* **97–8**, 410–415 (2002).
47. M. Avram, A. Avram, A. Bragaru, C. Bangtao, D.P. Poenar, and C. Iliescu: Low stress PECVD amorphous silicon carbide for MEMS applications. In *Proceedings of the Semiconductor Conference (CAS), 2010 International*, 2010; pp. 239–242.
48. F. Zhao, M.M. Islam, and C.F. Huang: Photoelectrochemical etching to fabricate single-crystal SiC MEMS for harsh environments. *Mater. Lett.* **65**(3), 409–412 (2011).
49. T.K. Hossain, S. MacLaren, J.M. Engel, C. Liu, I. Adesida, and R.S. Okojie: The fabrication of suspended micromechanical structures from bulk 6H-SiC using an ICP-RIE system. *J. Micromech. Microeng.* **16**(4), 751 (2006).
50. N. Rajan, M. Mehregany, C.A. Zorman, S. Stefanescu, and T.P. Kicher: Fabrication and testing of micromachined silicon carbide and nickel fuel atomizers for gas turbine engines. *J. Microelectromech. Syst.* **8**(3), 251–257 (1999).
51. T.H. Yoon, H.J. Lee, J. Yan, and D.P. Kim: Fabrication of SiC-based ceramic microstructures from preceramic polymers with sacrificial templates and lithographic techniques - A review. *J. Ceram. Soc. Jpn.* **114**(1330), 473–479 (2006).
52. T. Ishikawa, T. Namazu, K. Yoshiki, S. Inoue, and Y. Hasegawa: Polycarbosilane-derived silicon carbide MEMS component fabricated by slip casting with SU8 micro mold. In *Proceedings of the Micro Electro Mechanical Systems (MEMS), 2010 IEEE 23rd International Conference on*, 2010; pp. 416–419.
53. V. Cimalla, J. Pezoldt, and O. Ambacher: Group III nitride and SiC based MEMS and NEMS: Materials properties, technology and applications. *J. Phys. D: Appl. Phys.* **40**(20), 6386 (2007).
54. S. Pearton, F. Ren, Y-L. Wang, B. Chu, K. Chen, C. Chang, W. Lim, J. Lin, and D. Norton: Recent advances in wide bandgap semiconductor biological and gas sensors. *Prog. Mater. Sci.* **55**(1), 1–59 (2010).
55. S. Davies, T.S. Huang, M.H. Gass, A.J. Papworth, T.B. Joyce, and P.R. Chalker: Fabrication of GaN cantilevers on silicon substrates for microelectromechanical devices. *Appl. Phys. Lett.* **84**(14), 2566–2568 (2004).

https://doi.org/10.1557/jmr.2014.183 Published online by Cambridge University Press

56. Y. Wang, T. Sasaki, T. Wu, F. Hu, and K. Hane: Comb-drive GaN micro-mirror on a GaN-on-silicon platform. *J. Micromech. Microeng.* **21**(3), 035012 (2011).
57. F. Goericke, M. Chan, G. Vigevani, I. Izyumin, B. Boser, and A. Pisano: High temperature compatible aluminum nitride resonating strain sensor. In *Proceedings of the Solid-State Sensors, Actuators and Microsystems Conference (TRANSDUCERS), 2011 16th International*, 2011; pp. 1994–1997.
58. F.T. Goericke, G. Vigevani, I.I. Izyumin, B.E. Boser, and A.P. Pisano: Novel thin-film piezoelectric aluminum nitride rate gyroscope. In *Proceedings of the Ultrasonics Symposium (IUS), 2012 IEEE International*, 2012; pp. 1067–1070.
59. S.J. Pearton, B.S. Kang, K. Suku, F. Ren, B.P. Gila, C.R. Abernathy, L. Jenshan, and S.N.G. Chu: GaN-based diodes and transistors for chemical, gas, biological and pressure sensing. *J. Phys. Condens. Matter* **16**(29), R961 (2004).
60. L.A. Liew, W.G. Zhang, L.N. An, S. Shah, R.L. Luo, Y.P. Liu, T. Cross, M.L. Dunn, V. Bright, J.W. Daily, R. Raj, and K. Anseth: Ceramic MEMS - New materials, innovative processing and future applications. *Am. Ceram. Soc. Bull.* **80**(5), 25–30 (2001).
61. P. Colombo, G. Mera, R. Riedel, and G.D. Soraru: Polymer-derived ceramics: 40 Years of research and innovation in advanced ceramics. *J. Am. Ceram. Soc.* **93**(7), 1805–1837 (2010).
62. J. Bill and F. Aldinger: Precursor-derived covalent ceramics. *Adv. Mater.* **7**(9), 775–787 (1995).
63. L-A. Liew, Y. Liu, R. Luo, T. Cross, L. An, V.M. Bright, M.L. Dunn, J.W. Daily, and R. Raj: Fabrication of SiCN MEMS by photopolymerization of pre-ceramic polymer. *Sens. Actuators, A* **95**(2–3), 120–134 (2002).
64. L.A. Liew, W.G. Zhang, V.M. Bright, L.N. An, M.L. Dunn, and R. Raj: Fabrication of SiCN ceramic MEMS using injectable polymer-precursor technique. *Sens. Actuators, A* **89**(1–2), 64–70 (2001).
65. M. Schulz, M. Börner, J. Göttert, T. Hanemann, J. Haußelt, and G. Motz: Cross linking behavior of preceramic polymers effected by UV- and synchrotron radiation. *Adv. Eng. Mater.* **6**(8), 676–680 (2004).
66. M. Schulz: Polymer derived ceramics in MEMS/NEMS - A review on production processes and application. *Adv. Appl. Ceram.* **108**(8), 454–460 (2009).
67. P. Greil: Active-filler-controlled pyrolysis of preceramic polymers. *J. Am. Ceram. Soc.* **78**(4), 835–848 (1995).
68. P. Greil: Near net shape manufacturing of polymer derived ceramics. *J. Eur. Ceram. Soc.* **18**(13), 1905–1914 (1998).
69. V.M. Bright, R. Raj, M.L. Dunn, and J.W. Daily: Injectable ceramic microcast silicon carbonitride (SiCN) microelectromechanical system (MEMS) for extreme temperature environments with extension: Micro packages for nano-devices. Colorado University at Boulder Office of Contracts and Grants, 2004.
70. S. Jung, D. Seo, S.J. Lombardo, Z.C. Feng, J.K. Chen, and Y. Zhang: Fabrication using filler controlled pyrolysis and characterization of polysilazane PDC RTD arrays on quartz wafers. *Sens. Actuators, A* **175**, 53–59 (2012).
71. Y.P. Liu, L.A. Liew, R.L. Luo, L.N. An, M.L. Dunn, V.M. Bright, J. W. Daily, and R. Raj: Application of micro-forging to SiCN MEMS fabrication. *Sens. Actuators, A* **95**(2–3), 143–151 (2002).
72. D. Zhang, B. Su, and T.W. Button: Microfabrication of three-dimensional, free-standing ceramic MEMS components by soft moulding. *Adv. Eng. Mater.* **5**(12), 924–927 (2003).
73. D-H. Lee, K-H. Park, L-Y. Hong, and D-P. Kim: SiCN ceramic patterns fabricated by soft lithography techniques. *Sens. Actuators, A* **135**(2), 895–901 (2007).
74. D. Probst, H. Hoche, Y. Zhou, R. Hauser, T. Stelzner, H. Scheerer, E. Broszeit, C. Berger, R. Riedel, H. Stafast, and E. Koke: Development of PE-CVD Si/C/N: H films for tribological and corrosive complex-load conditions. *Surf. Coat. Technol.* **200**(1–4), 355–359 (2005).
75. S. Ma, B. Xu, G. Wu, Y. Wang, F. Ma, D. Ma, K. Xu, and T. Bell: Microstructure and mechanical properties of SiCN hard films deposited by an arc enhanced magnetic sputtering hybrid system. *Surf. Coat. Technol.* **202**(22–23), 5379–5382 (2008).
76. A.S. Bhattacharyya and S.K. Mishra: Micro/nanomechanical behavior of magnetron sputtered Si-C-N coatings through nano-indentation and scratch tests. *J. Micromech. Microeng.* **21**(1), 015011 (2011).
77. D.N. Hutchison, N.B. Morrill, Q. Aten, B.W. Turner, B.D. Jensen, L.L. Howell, R.R. Vanfleet, and R.C. Davis: Carbon nanotubes as a framework for high-aspect-ratio MEMS fabrication. *J. Microelectromech. Syst.* **19**(1), 75–82 (2010).
78. C.K. Malek and V. Saile: Applications of LIGA technology to precision manufacturing of high-aspect-ratio micro-components and -systems: A review. *Microelectron. J.* **35**(2), 131–143 (2004).
79. F. Ebrahimi, G.R. Bourne, M.S. Kelly, and T.E. Matthews: Mechanical properties of nanocrystalline nickel produced by electrodeposition. *Nanostruct. Mater.* **11**(3), 343–350 (1999).
80. K.J. Hemker and H. Last: Microsample tensile testing of LIGA nickel for MEMS applications. *Mater. Sci. Eng., A* **319**, 882–886 (2001).
81. J.G. Collins, M. Wright, and C.L. Muhlstein: Cyclic stabilization of electrodeposited nickel structural films. *J. Microelectromech. Syst.* **20**(3), 753–763 (2011).
82. T.J. Rupert and C.A. Schuh: Mechanically driven grain boundary relaxation: A mechanism for cyclic hardening in nanocrystalline Ni. *Philos. Mag. Lett.* **92**(1), 20–28 (2012).
83. T.R. Christenson, T.E. Buchheit, D.T. Schmale, and R.J. Bourcier: Mechanical and metallographic characterization of LIGA fabricated nickel and 80%Ni-20%Fe permalloy. *MRS Online Proc. Libr.* **518**(1), (1998).
84. T. Yamasaki: High-strength nanocrystalline Ni-W alloys produced by electrodeposition and their embrittlement behaviors during grain growth. *Scr. Mater.* **44**(8–9), 1497–1502 (2001).
85. T.E. Buchheit, S.J. Glass, J.R. Sullivan, S.S. Mani, D.A. Lavan, T.A. Friedmann, and R. Janek: Micromechanical testing of MEMS materials. *J. Mater. Sci.* **38**(20), 4081–4086 (2003).
86. S. Goods, J. Kelly, and N. Yang: Electrodeposited nickel-manganese: An alloy for microsystem applications. *Microsyst. Technol.* **10**(6–7), 498–505 (2004).
87. J. Kelly, S. Goods, and N. Yang: High performance nanostructured Ni-Mn alloy for microsystem applications. *Electrochem. Solid-State Lett.* **6**(6), C88–C91 (2003).
88. S.J. Hearne, M.P. de Boer, P.G. Kotula, C.W. Dyck, S.M. Foiles, D.M. Follstaedt, and T.E. Buchheit: *Novel In Situ Mechanical Testers to Enable Integrated Metal Surface Micro-Machines* (Sandia National Laboratories, 2005).
89. A.A. Talin, E.A. Marquis, S.H. Goods, J.J. Kelly, and M.K. Miller: Thermal stability of Ni-Mn electrodeposits. *Acta Mater.* **54**(7), 1935–1947 (2006).
90. G.D. Hibbard, K.T. Aust, and U. Erb: Thermal stability of electrodeposited nanocrystalline Ni–Co alloys. *Mater. Sci. Eng, A* **433**(1–2), 195–202 (2006).
91. M. Haj-Taieb, A. Haseeb, J. Caulfield, K. Bade, J. Aktaa, and K.J. Hemker: Thermal stability of electrodeposited LIGA Ni-W alloys for high temperature MEMS applications. *Microsyst. Technol.* **14**(9–11), 1531–1536 (2008).
92. S.J. Suresha, M. Haj-Taieb, K. Bade, J. Aktaa, and K.J. Hemker: The influence of tungsten on the thermal stability and mechanical behavior of electrodeposited nickel MEMS structures. *Scr. Mater.* **63**(12), 1141–1144 (2010).
93. A. Haseeb and K. Bade: LIGA fabrication of nanocrystalline Ni-W alloy micro specimens from ammonia-citrate bath. *Microsyst. Technol.* **14**(3), 379–388 (2008).

https://doi.org/10.1557/jmr.2014.183 Published online by Cambridge University Press

94. Y. Shacham-Diamand and Y. Sverdlov: Electrochemically deposited thin film alloys for ULSI and MEMS applications. *Microelectron. Eng.* **50**(1–4), 525–531 (2000).
95. P. Choi, T. Al-Kassab, F. Gärtner, H. Kreye, and R. Kirchheim: Thermal stability of nanocrystalline nickel-18 at.% tungsten alloy investigated with the tomographic atom probe. *Mater. Sci. Eng., A* **353**(1–2), 74–79 (2003).
96. C.A. Schuh, T.G. Nieh, and H. Iwasaki: The effect of solid solution W additions on the mechanical properties of nanocrystalline Ni. *Acta Mater.* **51**(2), 431–443 (2003).
97. C.F. Keimel, M.F. Aimi, S. Bansal, R.R. Corderman, K.V.S.R. Kishore, E.S. Reddy, A. Saha, K. Subramanian, P. Thakre, and A.D. Corwin: Switch Structure and Method. US Patent 2011/0067983, March 24, 2011.
98. R.L. Fleischer: Solid-solution hardening. In *The Strengthening of Metals*. (Reinhold Publishing Co., New York, NY, 1964).
99. T.J. Rupert, J.C. Trenkle, and C.A. Schuh: Enhanced solid solution effects on the strength of nanocrystalline alloys. *Acta Mater.* **59**(4), 1619–1631 (2011).
100. A.J. Detor, M.K. Miller, and C.A. Schuh: Solute distribution in nanocrystalline Ni-W alloys examined through atom probe tomography. *Philos. Mag.* **86**(28), 4459–4475 (2006).
101. A.J. Detor and C.A. Schuh: Microstructural evolution during the heat treatment of nanocrystalline alloys. *J. Mater. Res.* **22**(11), 3233–3248 (2007).
102. C. Borgia, T. Scharowsky, A. Furrer, C. Solenthaler, and R. Spolenak: A combinatorial study on the influence of elemental composition and heat treatment on the phase composition, microstructure and mechanical properties of Ni-W alloy thin films. *Acta Mater.* **59**(1), 386–399 (2011).
103. H. Miyamoto, S. Takehara, T. Uenoya, H. Fujiwara, and T. Goto: Nanocrystalline nickel dispersed with nano-size WO_3 particles synthesized by electrodeposition. *J. Mater. Sci.* **47**(12), 4798–4804 (2012).
104. J. Balaraju, N. Manikandanath, and V. William Grips: Phase transformation behavior of nanocrystalline Ni-W-P alloys containing various W and P contents. *Surf. Coat. Technol.* **206**(10), 2682–2689 (2013).
105. F. He, J. Yang, T. Lei, and C. Gu: Structure and properties of electrodeposited Fe-Ni-W alloys with different levels of tungsten content: A comparative study. *Appl. Surf. Sci.* **253**(18), 7591–7598 (2007).
106. G. Goward and D. Boone: Mechanisms of formation of diffusion aluminide coatings on nickel-base superalloys. *Oxid. Met.* **3**(5), 475–495 (1971).
107. R. Mevrel, C. Duret, and R. Pichoir: Pack cementation processes. *Mater. Sci. Technol.* **2**(3), 201–206 (1986).
108. J. Nicholls and D. Stephenson: High temperature coatings for gas turbines. *Met. Mater.* **7**(3), 156–163 (1991).
109. A.M. Hodge and D.C. Dunand: Synthesis of nickel-aluminide foams by pack-aluminization of nickel foams. *Intermetallics* **9**(7), 581–589 (2001).
110. D.C. Dunand, A.M. Hodge, and C. Schuh: Pack aluminisation kinetics of nickel rods and foams. *Mater. Sci. Technol.* **18**(3), 326–332 (2002).
111. S.J. Johnson, B. Tryon, and T.M. Pollock: Post-fabrication vapor phase strengthening of nickel-based sheet alloys for thermostructural panels. *Acta Mater.* **56**(17), 4577–4584 (2008).
112. S.J. Perez-Bergquist, N. Vermaak, and T.M. Pollock: High-temperature performance of actively cooled vapor phase strengthened nickel-based thermostructural panels. *AIAA J.* **49**(5), 1080–1086 (2011).
113. D.E. Burns, Y. Zhang, M. Teutsch, K. Bade, J. Aktaa, and K.J. Hemker: Development of Ni-based superalloys for microelectromechanical systems. *Scr. Mater.* **67**(5), 459–462 (2012).
114. D.M. Burns: Processing and Characterization of Ni-based Superalloy Micro-components and Films for MEMS Applications. Doctoral Dissertation, Department of Mechanical Engineering. Johns Hopkins University, Baltimore, MD, 2012.
115. H. Choe and D.C. Dunand: Synthesis, structure, and mechanical properties of Ni-Al and Ni-Cr-Al superalloy foams. *Acta Mater.* **52**(5), 1283–1295 (2004).
116. L. Liu, Y. Li, and F. Wang: Influence of grain size on the corrosion behavior of a Ni-based superalloy nanocrystalline coating in NaCl acidic solution. *Electrochim. Acta* **53**(5), 2453–2462 (2008).
117. L. Hanyi, W. Fuhui, X. Bangjie, and Z. Lixin: High-temperature oxidation resistance of sputtered micro-grain superalloy K38G. *Oxid. Met.* **38**(3), 299–307 (1992).
118. H. Lou, F. Wang, S. Zhu, B. Xia, and L. Zhang: Oxide formation of K38G superalloy and its sputtered micrograined coating. *Surf. Coat. Technol.* **63**(1–2), 105–114 (1994).
119. D.M. Burns, Y. Zhang, T.P. Weihs, and K.J. Hemker: Sputtered Ni-based superalloys for microscale devices. In *Proceedings of the Superalloys 2012: 12th International Symposium on Superalloys*, E.S. Huron, ed., Champion, PA, 2012; pp. 569–576.
120. A. Oradei-Basile and J.F. Radavich: A current TTT diagram for wrought alloy 718. *Superalloys* **718**(625), 325–335 (1991).
121. W.N. Sharpe: Murray lecture - Tensile testing at the micrometer scale: Opportunities in experimental mechanics. *Exp. Mech.* **43**(3), 228–237 (2003).
122. R.G. Azevedo, D.G. Jones, A.V. Jog, B. Jamshidi, D.R. Myers, C. Li, F. Xiao-An, M. Mehregany, M.B.J. Wijesundara, and A.P. Pisano: A SiC MEMS resonant strain sensor for harsh environment applications. *IEEE Sens. J.* **7**(4), 568–576 (2007).
123. C. Förster, V. Cimalla, V. Lebedev, J. Pezoldt, K. Brueckner, R. Stephan, M. Hein, E. Aperathitis, and O. Ambacher: Group III-nitride and SiC based micro- and nanoelectromechanical resonators for sensor applications. *Phys. Status Solidi A* **203**(7), 1829–1833 (2006).

https://doi.org/10.1557/jmr.2014.183 Published online by Cambridge University Press